Temperature-dependent photoluminescence of PbS quantum dots in glass: Evidence of exciton state splitting and carrier trapping

Maxim S. Gaponenko,[1,*] Andrey A. Lutich,[2] Nikolai A. Tolstik,[1] Alexei A. Onushchenko,[3] Alexander M. Malyarevich,[1] Eugene P. Petrov,[4] and Konstantin V. Yumashev[1]

[1]*Center for Optical Materials and Technologies, Belarusian National Technical University, Building 17, Nezavisimosti Avenue 65, 220013 Minsk, Belarus*

[2]*Photonics and Optoelectronics Group, Physics Department, Ludwig-Maximilians-Universität München, 80799 Munich, Germany*

[3]*Research and Technological Institute of Optical Materials Science, 193171 St. Petersburg, Russia*

[4]*Biophysics, BIOTEC, Technische Universität Dresden, Tatzberg 47/49, 01307 Dresden, Germany*

(Received 13 March 2010; revised manuscript received 18 June 2010; published 17 September 2010)

We report experimental evidence of the lowest exciton state splitting and carrier trapping in PbS quantum dots (QDs) in glass matrix. Our measurements of photoluminescence (PL) of PbS QDs using steady-state and time-resolved PL spectroscopy reveal strong temperature dependences of the PL intensity and decay kinetics. We find that consistent quantitative description of our experimental results can be achieved using a simple model taking into account the lowest 1S-1S exciton state splitting and multiphonon-assisted carrier trapping to states outside a PbS QD. Using our model, we estimate the lowest exciton splitting energy and lifetimes of the dark and bright exciton states of PbS QDs. Consistent with our model, the PL transition energy of PbS QDs deviates at higher temperatures from the one predicted based on the bulk PbS band-gap dependence due to the lowest 1S-1S exciton state splitting. Temperature-induced broadening of the PL spectrum of PbS QDs is explained by the exciton-phonon interaction.

DOI: 10.1103/PhysRevB.82.125320 PACS number(s): 78.67.Hc, 78.55.−m, 78.47.jd, 81.07.Ta

I. INTRODUCTION

The optical properties of semiconductor nanocrystals or quantum dots (QDs) have been extensively investigated over the past decade and still attract a growing interest from both fundamental and applied points of view. These low-dimensional systems bridge the gap between single molecules and bulk solid state, providing an opportunity to trace the evolution of electronic and optical properties of the matter from small atomic clusters to bulk solids. Because of quantum confinement, QDs possess size-dependent discrete exciton energy levels.[1–3] This feature allows for tuning of the spectral position of the absorption and emission bands of QDs by varying their size and makes them promising for tunable absorbers and emitters in applications such as light-emitting devices[4–7] and biomedical fluorescent labeling.[8–13] Following the extensive investigation of optical properties of CdS and CdSe QDs during the past years, rocksalt-structured lead sulfide (PbS) QDs have recently emerged as an interesting semiconductor low-dimensional system. From the fundamental point of view, the narrow band gap (0.42 eV at room temperature),[14] large (17.4 nm) exciton Bohr radius,[15] and nearly equivalent electron and hole effective masses[14] make them attractive candidates for investigating strong quantum confinement effects. From the technological perspective, PbS QDs are of interest because they are among the few materials that can provide tunable electronic transitions in the range of $1-3$ μm, thus allowing for controlled light absorption and emission at these important near-infrared (IR) wavelengths.

In lead salt (PbS, PbSe, and PbTe) QDs the lowest-energy excitonic manifold (1S-1S) originates from the four equivalent L points in the Brillouin zone. Thus, one may expect its fourfold degeneracy (in addition to the Kramers degeneracy).[16] Unfortunately, accurate theoretical calculations of the energy level structure in PbS QDs have not been carried out up to now. At the same time, a recent atomistic pseudopotential calculation of PbSe QDs energy levels has revealed a fine structure of the lowest exciton state.[17] The electron-hole exchange interaction and spin-orbit coupling lead to the appearance of the nondegenerate lower-energy *dark* exciton state, followed by the higher-energy threefold degenerate *bright* exciton state in PbSe QDs. Optical transitions to and from the dark exciton state are forbidden within the electric dipole approximation, and radiative recombination from this state can only take place via the emission or absorption of phonons.[18,19] If such a splitting occurs, the radiative rate is expected to depend on the thermal activation rate between the dark and bright states. The temperature dependence of the luminescence decay in PbS QDs in glass recently reported in Ref. 20 was suggested as an argument in support of the above model, although, quite surprisingly, the steady-state photoluminescence (PL) intensity for the same samples was found to have only a weak, nonmonotonic temperature dependence. By contrast, a tenfold increase in the steady-state luminescence intensity with a decrease in temperature from 295 to 50 K was observed in thiol-capped PbS QDs (Ref. 21) and explained by the thermally activated trapping of carriers to the defects; the latter study, however, presented no data for PL decay times. In view of these somewhat contradictory and incomplete results, it is therefore reasonable to expect that a proper understanding of the temperature-dependent luminescence properties of PbS QDs requires a model which should provide an adequate simultaneous description of the temperature dependences of both the steady-state PL intensity and PL decay times. We believe that such a model should simultaneously take into consideration both the lowest exciton state splitting and the carrier trapping.

It is well known that PL transition energy in semiconductor QDs is temperature dependent. At the same time, no clear theoretical prediction for this dependence has been published. In the absence of a theoretical expression for this dependence, a number of authors have found that a satisfactory description of experimental data for QDs (CdSe/ZnS, CdSe/CdS, and InP/ZnS) can be achieved using the theoretical dependences of the band-gap energy in bulk semiconductors.[22–24] On the other hand, it is still unclear, whether this approach is universal enough to provide an adequate description of experimental data for QDs of other semiconductor compounds.

In the present work, we investigate the steady-state and time-resolved PL of PbS QDs in a glass matrix and propose a model accounting for the exciton splitting and carrier trapping at defect sites, showing excellent agreement with the experimental results on the temperature-dependent PL intensity and decay kinetics. Additionally, we demonstrate that, while at lower temperatures the known empirical relations for bulk semiconductors can describe the temperature dependence of the PL transition energy, they fail at higher temperatures because of the lowest 1S-1S exciton state splitting. The observed temperature-induced broadening of the PL spectrum of PbS QDs is explained by the exciton-phonon interaction.

II. EXPERIMENT

A silicate glass sample doped with PbS QDs was prepared using the system compound SiO_2-Al_2O_3-NaF-Na_2O-ZnO. The glass batch melting technique with a double-stage heat treatment procedure was similar to those reported elsewhere.[25,26] The technique provides controllable growth of QDs with the size distribution of 5–7 %. Room-temperature absorption spectrum of the glass doped with PbS QDs was recorded on a Cary 500 spectrophotometer (Varian). The transition energy corresponding to the maximum of the first exciton absorption band was used to estimate the average size of QDs in the sample by fitting to a sizing curve for PbS QDs in silicate glass from Ref. 27. The evaluated mean radius of QDs is 2.5 nm.

Steady-state PL measurements were carried out using a Jobin-Yvon Fluorolog-3 spectrometer equipped with a Hamamatsu near-infrared photomultiplier tube. The spectral response of the detection system was calibrated using broadband emission from a tungsten lamp. The spectral widths of the slits were set to 2 nm. For the temperature-dependent measurements, the sample was mounted in a temperature-controllable helium flow cryostat (Oxford Instruments). The excitation wavelength was set to 400 nm.

An optical parametric oscillator (LOTIS TII) pumped by the third harmonic (355 nm) of a *Q*-switched Nd:YAG laser (LOTIS TII) was used as an excitation source in the time-resolved PL measurements. The system provided spectrally tunable pulses with duration of 10 ns at a repetition rate of 10 Hz. The PbS QDs sample mounted in the cryostat was excited to the maximum of its first exciton absorption band at 1.025 eV (1210 nm). The PL was collected by lenses and spectrally selected using a 0.3 m monochromator (SPEX) to a bandwidth of 5 nm at the 0.91 eV (1360 nm). PL decay traces were acquired using a Hamamatsu near-IR photomultiplier tube and a 500 MHz bandwidth digital oscilloscope (LeCroy). The excitation radiation fluence at the sample was ~ 0.05 MW/cm^2 (the diameter of the excitation spot at the sample was ~ 1 mm), which is about two orders of magnitude lower than the absorption saturation intensity of 2 MW/cm^2 measured in an independent experiment (data not shown). Thus, the linear excitation regime was ensured in our experiments.

PL decay kinetics were found to exhibit complex nonsingle exponential decays and therefore were analyzed by reconstructing the underlying distributions of decay times with minimum *a priori* assumptions on the PL decay law. In this approach, the PL decay law is represented by a distribution of decay times $f(\tau)$,

$$I(t) = \int_{\tau_{\min}}^{\tau_{\max}} f(\tau)\exp(-t/\tau)d\tau. \quad (1)$$

Taking into account that the measured PL kinetics $D(t)$ is a convolution of the genuine decay law $I(t)$ and the response function of the detection system $R(t)$, the problem of the PL decay analysis is reduced to the solution of the integral equation,

$$\int_0^t R(t-t')\int_{\tau_{\min}}^{\tau_{\max}} f(\tau)\exp(-t'/\tau)dt'd\tau = D(t) \quad (2)$$

with respect to $f(\tau)$. A discretized version of this ill-posed inverse problem, where integral Eq. (1) is approximated by the sum $\Sigma_{i=1}^{n} f_i \exp(-t/\tau_i)$ with the fixed decay times $\tau_i \in [\tau_{\min}, \tau_{\max}]$, was solved using a regularization procedure described elsewhere.[28] The lifetime distributions were reconstructed using $n=100$ exponential terms with decay times uniformly distributed on the logarithmic scale in the range of 0.05–200 μs. The accuracy of experimental PL data fitting is assessed by analyzing the residuals and their autocorrelation function. The mean decay time $\langle\tau\rangle$ is calculated as

$$\langle\tau\rangle = \sum (f_i\tau_i^2)/\sum (f_i\tau_i). \quad (3)$$

III. RESULTS AND DISCUSSION

A. Room-temperature absorption and emission

Figure 1 shows the absorption and PL spectra of the PbS QDs sample at the room temperature (293 K). The maximum of the first exciton absorption band is located at 1.025 eV (1210 nm). The PL spectrum has a full width at half maximum (FWHM) of 105 meV and is centered at 0.95 eV (1305 nm), which corresponds to a nonresonant Stokes shift of 75 meV. The FWHM of the room-temperature PL spectrum measured for an ensemble of PbS QDs in our samples is smaller than 180–200 meV reported previously for ensemble measurements[20,29,30] and is close to 90–130 meV reported recently in ensemble measurements on thiol-capped PbS QDs.[31] For single PbS QDs, the FWHM value of ~ 100 meV was reported,[32] and the large homogeneous linewidth in PbS QDs was explained by the ultrafast exciton

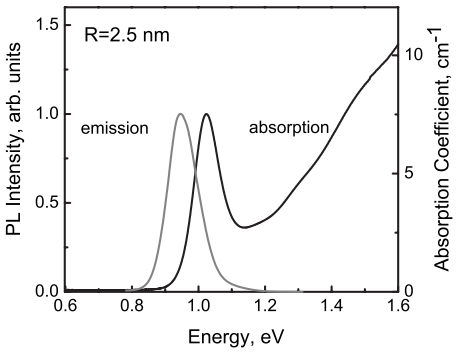

FIG. 1. Room-temperature absorption and photoluminescence spectra of PbS QD sample used in our experiments. The estimated mean radius of PbS QDs is 2.5 nm.

dephasing.[33] Thus, the FWHM value of 105 meV obtained for our sample is consistent with the narrow size distribution of nanocrystals.

B. Temperature-dependent steady-state photoluminescence

PL spectra of the PbS QD sample exhibit a strong temperature dependence in the range of 10–300 K (Fig. 2). The temperature decrease leads to the shift of the emission maximum to lower energies and pronounced growth of the PL intensity (Figs. 2 and 3). The appearance of an additional low-intensity wide emission band at higher energies can also be observed. We found that all PL spectra can be well approximated by a sum of two Gaussians. The band making the major contribution to the PL spectra shifts to higher energies and broadens with an increase in the temperature. The second low-intensity band does not demonstrate a pronounced temperature dependence, exhibiting a peak position at 1.0–1.04 eV and FWHM values in the range of 110–170 meV within the whole temperature range. These results suggest that, while the first emission band reflects the intrinsic properties of QDs, the second one originates from trap states. Glasses are amorphous solid solutions and, therefore, the formation of defect states in the strained matrix volume surrounding a QD surface can be expected. The importance of these trap states in the exciton relaxation was pointed out in the experiments on the resonant femtosecond pump-probe

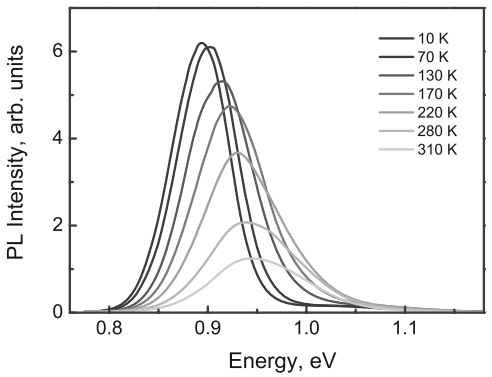

FIG. 2. Temperature-dependent photoluminescence spectra of PbS QDs.

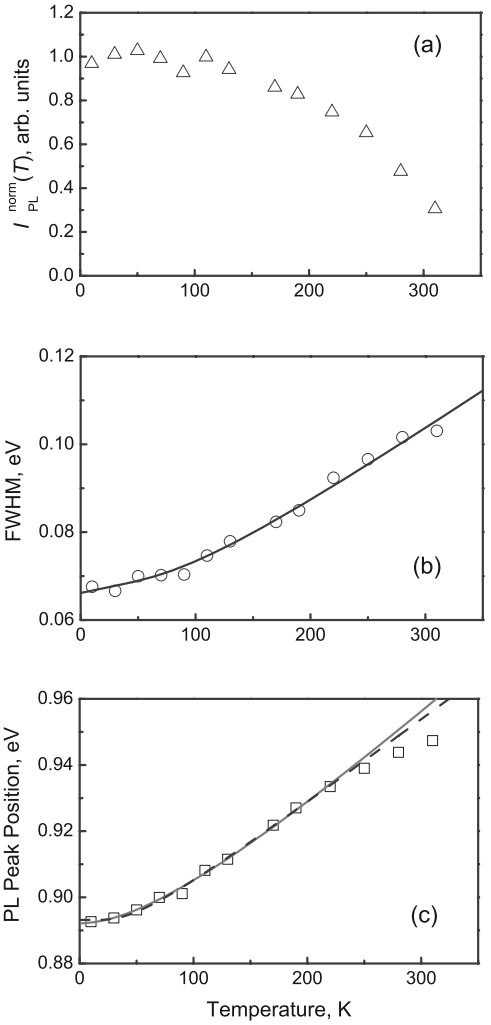

FIG. 3. Temperature dependences of the (a) integral intensity, (b) full width at half maximum, and (c) peak spectral position of PbS QDs intrinsic exciton photoluminescence band. Symbols represent experimental data. Solid curve in (b) is a least-squares fit using Eq. (4) ($\Gamma_{inh}=66\pm1$ meV, $\sigma=54\pm12$ μeV/K, $\gamma=39\pm6$ meV). Solid curve in (c) is a least-squares fit using Eq. (5) [$E_{1S\text{-}1S}(0)=0.892\pm0.001$ eV, $\alpha_{1S\text{-}1S}=320\pm4$ μeV/K, $\beta=143\pm48$ K]; dashed curve in (c) is a least-squares fit using Eq. (6) [$E_{1S\text{-}1S}(0)=0.893\pm0.001$ eV, $S=1.48\pm0.07$, and $\langle E_{ph}\rangle=11.7\pm1.7$ meV].

spectroscopy of CdTe,[34] CdSSe,[35] and CdS (Ref. 36) QDs in glasses and time-resolved photoluminescence spectroscopy of colloidal CdSe QDs.[37] Additionally, emission from trap states was observed for QDs in various environments (see, e.g., Refs. 38–41). Several trap-related emission bands have been reported for PbS QDs in polyvinyl alcohol.[40] These literature data confirm our assignment of the lower-energy temperature-dependent narrower band to the intrinsic exciton PL of PbS QDs and the higher-energy temperature-independent wider band to trap states emission. Carriers can be trapped to these states from the 1S-1S exciton state, as well as from the higher lying states to which they are promoted by the optical excitation. In what follows, we will present and discuss only the temperature dependence of the intrinsic exciton PL.

Figure 3(b) shows the FWHM of the intrinsic PbS QDs exciton emission as a function of temperature. The temperature dependence of the FWHM due to the exciton-phonon interactions can be described by the following equation:[42,43]

$$\mathrm{FWHM}(T) = \Gamma_{inh} + \sigma T + \gamma N_{\mathrm{LO}}(T), \tag{4}$$

where temperature-independent inhomogeneous contribution Γ_{inh} represents a distribution (due to QD size, shape, and environment variations) of linewidths of single QDs in the ensemble at $T \to 0$; σ is an exciton-acoustic-phonon coupling coefficient; γ is a temperature-independent linewidth parameter characterizing the total linewidth due to exciton-LO-phonon interactions; and $N_{\mathrm{LO}}(T)=[\exp(E_{\mathrm{LO}}/k_BT)-1]^{-1}$ is the Bose-Einstein distribution of LO phonons. Originally, Eq. (4) was derived to analyze the temperature dependence of exciton linewidths in bulk semiconductors.[42] Later, the relation of similar form was introduced to describe the temperature dependence of exciton luminescence linewidths in semiconductor quantum wells.[43] At present, Eq. (4) is widely used to describe PL linewidth in semiconductor QDs (see, e.g., Refs. 22–24 and 44). In our calculations we set the LO-phonon energy $E_{\mathrm{LO}}=26.6$ meV. This value corresponds to the center of the peak in the Raman-scattering spectrum of PbS QDs with diameter of 3 nm, which was assigned to the lowest-order optical mode.[45] Equation (4) provides an accurate description of the PL FWHM with the fitting parameters $\Gamma_{inh}=66\pm1$ meV, $\sigma=54\pm12$ μeV/K, and $\gamma=39\pm6$ meV [Fig. 3(b)]. The value of Γ_{inh} is in a good agreement with the one obtained from the Raman-scattering data measured at 4.2 K for an ensemble of 3 nm PbS QDs with a size distribution of $\pm4\%$ reported in Ref. 46, where the best fits were obtained with the linewidth of inhomogeneous distribution $\Gamma_{inh}=50-87$ meV. Unfortunately, we failed to find any data on σ and γ coefficients for bulk PbS or PbS QDs in the literature to directly compare with our data. However, our values are in the range of those reported for CdSe QDs ($\sigma=71\pm9$ μeV/K, $\gamma=21\pm7$ meV) (Ref. 22) and CdTe QDs ($\sigma=33\pm6$ μeV/K, $\gamma=18.3\pm0.9$ meV) (Ref. 47) of the same size and PbSe QDs with diameter of 4.1 nm ($\sigma=80$ μeV/K, $\gamma=40$ meV).[48] The higher values of γ obtained for lead salt QDs can indicate stronger exciton-LO-phonon coupling in these systems, which are characterized by noticeably stronger quantum confinement due to the larger exciton Bohr radius. However, the origin of the coupling strength increase is not yet clear. We should note, that despite the intensive experimental and theoretical investigation there is still no consensus on the influence of the confinement level on the exciton-phonon coupling strength [its enhancement, attenuation (see Refs. 49 and 50, and references therein) or nonmonotonic change[50] with the decrease in a QD size were reported].

The temperature dependence of the PL peak position of the PbS QDs is shown in Fig. 3(c). The redshift of the PL peak with a decrease in temperature reflects a reduction in the PbS QD energy band gap, which is, strictly speaking, the energy of the lowest allowed 1S-1S exciton state. No detailed theory that would allow for an accurate description of the temperature dependence of the lowest exciton energy in QDs is currently available. On the other hand, it is widely accepted that, in the absence of temperature-dependent absorption data, the temperature dependence of the PL transition energy in QDs can be used as a proxy for the temperature dependence of the QD bang-gap energy. This approach implies temperature-independent Stokes shift, which is a reasonable assumption. Based on this assumption, it is common to analyze experimental data on the temperature-dependent QD PL transition energy using phenomenological expressions originally introduced to describe the band-gap temperature dependence in bulk semiconductors.[22–24,48,51,52] In the present work we adopt the same approach.

The temperature dependence of the PL peak position can be well described for $T \leq 220$ K by either of the two following phenomenological expressions. The first one is a relation introduced by Varshni,[53]

$$E_g(T) = E_g(0) + \alpha\frac{T^2}{T+\beta}, \tag{5}$$

where $E_g(0)$ represents the band gap at $T=0$ K [in the case of QDs the E_g should be understood as the energy of the lowest 1S-1S exciton state which is the sum of the bulk band-gap energy E_g and quantum confinement energy E_{conf}, and therefore the notation $E_{1S\text{-}1S}(0)$ will be used below for QDs]; β is a constant of the order magnitude of the semiconductor material Debye temperature Θ_{D}; and α is the band-gap energy temperature coefficient. We use the second term with the plus sign (rather than with the minus sign, as it was in the original paper) because the PbS band-gap energy rises with an increase in temperature, in contrast to most of semiconductor materials. The fit of PbS QDs PL peak position using Eq. (5) is presented in Fig. 3(c). A good agreement with the experimental data for $T \leq 220$ K is observed. The fitting parameters are $E_{1S\text{-}1S}(0)=0.892\pm0.001$ eV, $\alpha_{1S\text{-}1S}=320\pm4$ μeV/K, and $\beta=143\pm48$ K. The value of β is similar to the Debye temperature of bulk PbS obtained from x-ray Bragg reflection data ($\Theta_{\mathrm{D}}=145$ K).[14,54] The obtained temperature coefficient $\alpha_{1S\text{-}1S}$ is smaller than the bulk value $dE_g/dT=520$ μeV/K.[54] This can be expected since the theoretical estimation of $dE_{1S\text{-}1S}/dT$ for PbS QDs with the mean radius of 2.5 nm in phosphate glass gives the value of ~50 μeV/K.[55]

The second relation for a band-gap temperature dependence was proposed by O'Donnell and Chen,[56]

$$E_g(T) = E_g(0) + S\langle E_{ph}\rangle[\coth(\langle E_{ph}\rangle/2k_BT) - 1], \tag{6}$$

where $\langle E_{ph}\rangle$ is an average phonon energy and S is a dimensionless coupling constant usually referred to as Huang-Rhys parameter. Also in this case the second term is used with the plus sign, rather than the minus sign in the original work. The fit of PbS QDs PL peak position using Eq. (6) is presented in Fig. 3(c). The fitting parameters are $E_{1S\text{-}1S}(0)=0.893\pm0.001$ eV, $S=1.48\pm0.07$, and $\langle E_{ph}\rangle=11.7\pm1.7$ meV. The obtained average phonon energy $\langle E_{ph}\rangle=11.7$ meV is close to the bulk value of 14 meV.[14] The Huang-Rhys parameter is reasonably close to the value of ~0.7 determined for 1.5 nm radius PbS QDs using resonant Raman spectroscopy.[46]

Although the above dependences accurately describe the temperature-induced shift of the PL peak position for $T \leq 220$ K, both of them clearly fail to do so at higher temperatures, $T \geq 250$ K. Such a behavior can be attributed to a presence of two different energetically separated emitting states with a thermally activated transition between them, which is a result of the exciton dark-bright-state splitting. At lower temperatures, the number of excitons occupying the dark state increases and emission from this state provides a major contribution to the PL signal.

C. Temperature-dependent photoluminescence decay

PL decays recorded within the range of temperatures from 10 to 300 K are clearly nonsingle-exponential with the characteristic PL decay time increasing with a decrease in temperature [Fig. 4(a)]. The distributions of decay times corresponding to these PL decays consistently show three peaks with temperature-dependent positions [Fig. 4(b)]. However, the finite accuracy of the experimental data does not allow us to rule out a possibility that the complex PL decays are due to continuous distribution of decay times. To unambiguously discriminate between these two scenarios, much higher accuracy of PL decay measurements is required. Interpretation of the structure of the lifetime distributions thus requires a special detailed study and is outside the scope of the present work. In what follows, we will use the mean decay time $\langle \tau \rangle$ [Eq. (3)] as a single parameter characterizing the PL decay at a given temperature.

The mean PL lifetime $\langle \tau \rangle$ at the room temperature is 2.7 μs [Fig. 4(c)], which agrees well with experimentally measured values for PbS and PbSe QDs reported by different groups.[30,57–59] The long PL lifetimes in lead chalcogenide QDs at the room temperature are mainly attributed to the small oscillator strength of the bright exciton state[17] and large local field screening factor due to a high dielectric constant of the QD core material[17,60] [bulk values are $\varepsilon(\infty) = 17.2$ for PbS and $\varepsilon(\infty) = 23.9$ for PbSe].[14]

D. A model combining temperature dependences of photoluminescence intensity and decay time

We propose the following simple model to describe the temperature-dependent exciton photoluminescence in PbS QDs, which can be summarized using the sketch presented in Fig. 5. The fine structure of the lowest 1S-1S exciton state is represented by the *bright* and *dark* states with the radiative decay rates k_{bright} and k_{dark}, respectively, separated by the energy gap ΔE. We assume the same degeneracy for both states since the exact values have been not reported for PbS QDs. The relaxation rates of 1S-1S exciton fine structure states in PbS QDs of similar size were recently estimated to be >1 ps^{-1}.[61] Therefore we assume the Boltzmann distribution of excitons in the bright and dark states in the QD ensemble. The difference in radiative decay rates k_{bright} and k_{dark}, along with the thermally activated carrier trapping to the states outside the core of a QD are assumed to be the main reasons for the observed PL thermal quenching at high temperatures [see Figs. 2 and 3(a)] and PL lifetime increase at low temperatures (Fig. 4). We assume that trapping occurs

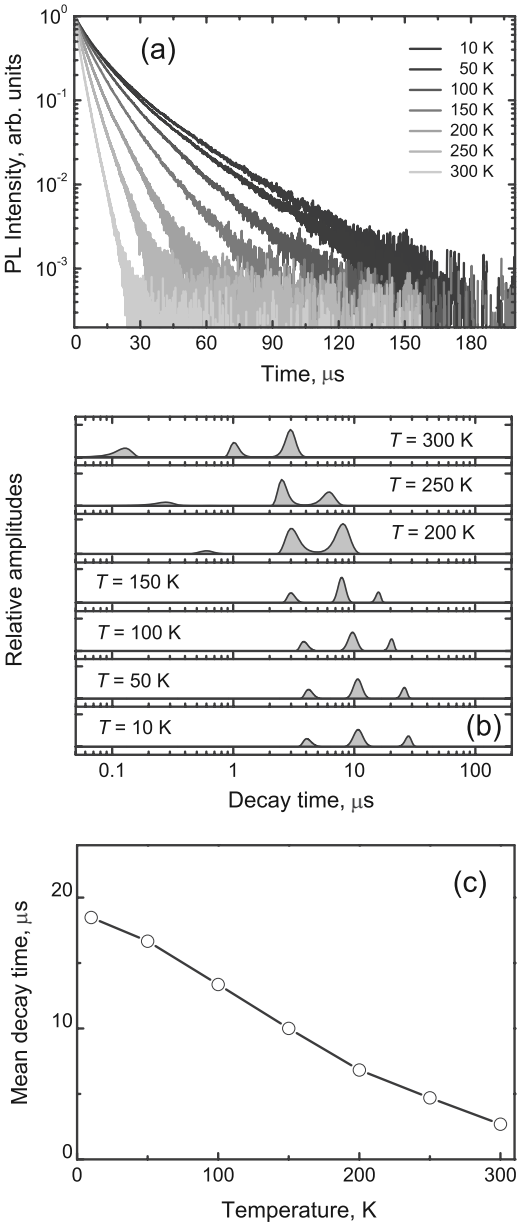

FIG. 4. (a) Temperature-dependent photoluminescence decay kinetics, (b) distributions of PL decay times, and (c) mean PL decay times calculated according to Eq. (3). Solid line in (c) is a guide for the eyes.

from dark and bright states with absorption of m and n phonons ($m > n$), respectively. Then, the following rate equation for the total number of excitons N in the ensemble of potentially emitting QDs can be written as

$$\frac{dN}{dt} = -(k_{bright} + \kappa_{bright,n})N_1 - (k_{dark} + \kappa_{dark,m})N_2,$$

$$N_1/N_2 = \exp(-\Delta E/k_B T),$$

$$N = N_1 + N_2, \tag{7}$$

where N_1 and N_2 are the populations of bright and dark states, which obey the Boltzmann distribution and together

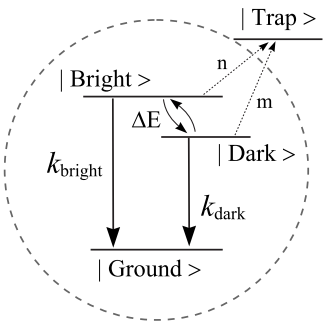

FIG. 5. A schematic representation of the exciton relaxation processes described by Eq. (7) (see text for details).

constitute the total number of excitons; k_{bright} and k_{dark} are their radiative decay rates, $\kappa_{bright,n}$ and $\kappa_{dark,m}$ are nonradiative relaxation rates. We assume that the corresponding probabilities $\kappa_{bright,n}$ and $\kappa_{dark,m}$ of nonradiative relaxation from the bright and dark states to a trap state with absorption of n and m phonons with energy E_{ph} can be expressed as $\kappa_{bright,n}=k_0[\exp(E_{ph}/k_BT)-1]^{-n}$ and $\kappa_{dark,m}=k_0[\exp(E_{ph}/k_BT)-1]^{-m}$, respectively, where k_0 is a rate constant characterizing the efficiency of the thermally induced nonradiative relaxation to trap states. By solving Eq. (7), we obtain the following expression for the temperature dependence of the PL decay time:

$$\tau(T) = 1/k(T) = \frac{1+a}{ak_{bright} + k_{dark} + k_0[a(b-1)^{-n} + (b-1)^{-m}]} \tag{8}$$

with the temperature-dependent coefficients $a(T)=\exp[-(m-n)E_{ph}/k_BT]$ and $b(T)=\exp(E_{ph}/k_BT)$ [note that $\Delta E=(m-n)E_{ph}$]. Taking into account that at low temperatures the thermally activated carrier trapping vanishes, and as a result the PL intensity reaches its maximum value I_0, one can express the normalized PL integral intensity as follows:

$$I_{\mathrm{PL}}^{norm}(T) = I_{\mathrm{PL}}(T)/I_0 = \frac{k_{rad}(T)}{k_{rad}(T) + k_{nonrad}(T)}. \tag{9}$$

The radiative $k_{rad}(T)$ and nonradiative $k_{nonrad}(T)$ decay rates can be obtained from Eq. (7) as

$$k_{rad}(T) = (ak_{bright} + k_{dark})/(1+a), \tag{10}$$

$$k_{nonrad}(T) = k_0[a(b-1)^{-n} + (b-1)^{-m}]/(1+a). \tag{11}$$

By combining Eqs. (9)–(11), we obtain the following relation for the temperature dependence of the normalized PL integral intensity:

$$I_{\mathrm{PL}}^{norm}(T) = I_{\mathrm{PL}}(T)/I_0 = \frac{ak_{bright} + k_{dark}}{ak_{bright} + k_{dark} + k_0[a(b-1)^{-n} + (b-1)^{-m}]}. \tag{12}$$

Comparing Eqs. (8), (10), and (12), one can see that the ratio of the PL decay time to the normalized PL integral intensity gives the radiative exciton lifetime $\tau_{rad}(T)$,

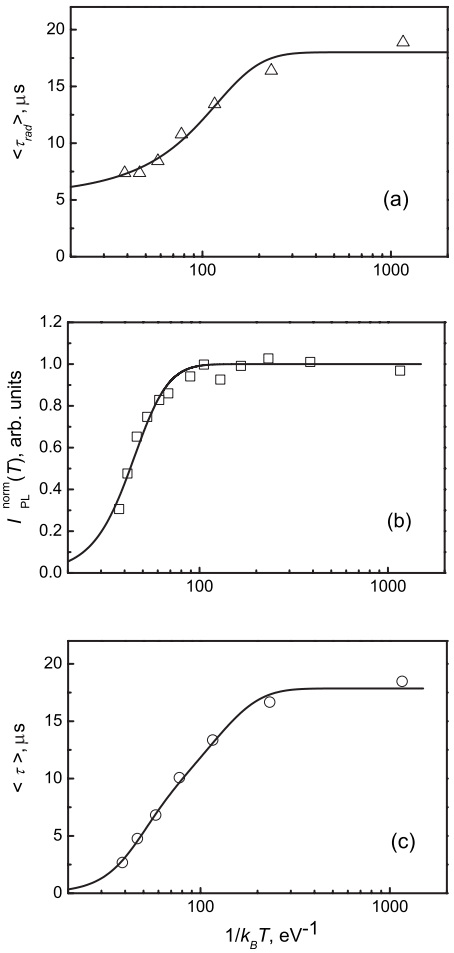

FIG. 6. (a) Exciton radiative lifetime (open symbols) and its fit using Eq. (13). The fitting parameters are $k_{bright}=0.33\pm0.04$ μs^{-1}, $k_{dark}=0.056\pm0.001$ μs^{-1}, and $(m-n)=0.82\pm0.01$. (b) Temperature dependence of normalized exciton PL integral intensity. Symbols are experimental data, solid curve is a least-squares fit using Eq. (12). (c) Temperature dependence of the mean PL decay time. Symbols are experimental data, solid curve is a least-squares fit using Eq. (8). The fitting parameters in (b) and (c) are $k_0=1.07\pm0.18$ μs^{-1} and $m=3.05\pm0.19$.

$$\tau_{rad}(T) = 1/k_{rad}(T) = \tau(T)/I_{\mathrm{PL}}^{norm}(T) = \frac{1+a}{ak_{bright} + k_{dark}}. \tag{13}$$

Based on the experimentally accessible data, the following estimate of the radiative exciton lifetime can be obtained using Eq. (13): $\langle\tau_{rad}(T)\rangle=\langle\tau(T)\rangle/I_{\mathrm{PL}}^{norm}(T)$, where $\langle\tau(T)\rangle$ is the experimentally measured mean PL decay time and $I_{\mathrm{PL}}^{norm}(T)$ is the experimentally measured PL intensity normalized by its value at low temperatures.

At this moment we are ready to apply our model to analyze our experimental data on PbS QD photoluminescence. First, we analyze the temperature dependence of the experimental estimate of the radiative exciton lifetime $\langle\tau_{rad}(T)\rangle$ [Fig. 6(a)], which, within the framework of our model, should depend only on three model parameters: k_{bright}, k_{dark}, and difference $(m-n)$. To do that, we set E_{ph} equal to the LO-phonon energy $E_{\mathrm{LO}}=26.6$ meV.[45] The best fit was found

for the following set of parameters: $k_{bright}=0.33\pm0.04$ μs^{-1}, $k_{dark}=0.056\pm0.001$ μs^{-1}, and $(m-n)=0.82\pm0.10$ [Fig. 6(a)]. The corresponding exciton emission lifetimes and energy splitting of the dark and bright states can be estimated as $\tau_{dark}=17.9$ μs, $\tau_{bright}=3$ μs, and $\Delta E=21.8\pm3.2$ meV.

As a second step, we apply our model to the experimental data on temperature dependences of PL intensity and decay time [Figs. 6(b) and 6(c)]. These data sets were fitted independently using Eqs. (8) and (12), accordingly, with the parameters k_{dark}, k_{bright}, and $(m-n)$ fixed at their values obtained in the above analysis of the radiative exciton lifetimes. The best fits produced two close sets of parameters: $k_0=1.03\pm0.22$ μs^{-1} and $m=3.0\pm0.2$ for the $I_{PL}^{norm}(T)$ data set; $k_0=1.37\pm0.49$ μs^{-1} and $m=3.35\pm0.39$ for the $\langle\tau(T)\rangle$ data set [Figs. 6(b) and 6(c)]. The simultaneous fitting of the $I_{PL}^{norm}(T)$ and $\langle\tau(T)\rangle$ data sets was also carried out and, as expected, resulted in nearly the same parameter values: $k_0=1.07\pm0.18$ μs^{-1} and $m=3.05\pm0.19$.

As a third step, to verify the stability and reproducibility of the model parameters, we carried out the simultaneous fitting of the $I_{PL}^{norm}(T)$ and $\langle\tau(T)\rangle$ experimental data sets using Eqs. (8) and (12) with five variable parameters k_{bright}, k_{dark}, k_0, m, and n. The best fit was found for the parameter values $k_{bright}=0.30\pm0.05$ μs^{-1}, $k_{dark}=0.056\pm0.001$ μs^{-1}, $k_0=0.99\pm0.19$ μs^{-1}, $m=2.98\pm0.20$, and $n=2.21\pm0.20$, which are very close to the results reported above, thus confirming the above data analysis and consistency of our model.

The estimated value of the bright-dark state energy gap $\Delta E=21.8$ meV exceeds the values of 1–16 meV previously reported for CdSe QDs (see, e.g., Ref. 62, and references therein). This can be explained by the enhanced electron-hole exchange interaction in lead chalcogenide QDs for which the levels of quantum confinement are noticeably higher then for QDs of II-VI semiconductors due to the larger exciton Bohr radius (the theoretically calculated value of $\Delta E=120$ meV for 2.7-nm-diameter PbS QDs was reported).[32] The difference between the obtained values of τ_{dark} and τ_{bright} is not as appreciable as for QDs of II-VI semiconductors, which is typically about two orders of magnitude.[62–64] The spin-orbit coupling and QD shape asymmetry dramatically alter the excitonic fine structure of lead chalcogenide QDs by heavily intermixing of the pure exciton spin states.[17] Therefore, we conclude that the bright and dark states in PbS QDs have considerable admixture of both characters. This can also be the reason of long (microsecond time range) room-temperature PL lifetimes in PbS QDs. Thus, our simple model provides an accurate consistent description of experimental data sets obtained from two different independent experiments using the same set of parameters with physically reasonable values.

IV. CONCLUSIONS AND OUTLOOK

In conclusion, we studied the photoluminescence properties of PbS QDs embedded in a glass matrix in the temperature range of 10–300 K and found that the PL intensity, lifetime, linewidth, and spectral position are all strongly temperature dependent. We developed a simple model for PbS QD photoluminescence, which combines the thermally induced carrier trapping to the states outside the QD core, which occurs via multiphonon absorption, and the bright-dark exciton fine structure splitting. This model accurately describes the temperature dependences of the PL intensity and decay time in PbS QDs. Using our simple model, we estimated the lowest exciton state splitting energy in 2.5 nm radius PbS QDs to be $\Delta E=21.8$ meV. The values of radiative lifetimes of the bright and dark states were estimated as 3 μs and 17.9 μs, respectively. Additionally, we investigated the temperature dependence of the PL transition energy and demonstrated that it can be described within the wide temperature range with the use of the relations introduced for bulk semiconductor band-gap energy, although at higher temperatures these relations fail due to the splitting of the lowest 1S-1S exciton state. The observed broadening of the PL linewidth with temperature is explained by the exciton-phonon coupling mechanism.

The better understanding of the trap-related exciton recombination in these nanostructures requires conducting similar experiments using PbS QDs capped with different agents, which can be produced, e.g., using colloidal nanocrystal synthesis. This approach can help to distinguish relaxation channels of electrons and holes. Additionally, we believe that temperature-dependent time-resolved measurements of differential absorption spectra using the pump-probe spectroscopy technique will be of help to create a unified picture of carrier relaxation pathways in PbS QDs. These data will advance the rational design of PbS QDs-based materials with specific properties for applications in the near infrared.

ACKNOWLEDGMENTS

The authors thank Günter Huber, Institute for Laser Physics, University of Hamburg for kindly providing access to the experimental facilities for temperature-dependent luminescence lifetime measurements. M.S.G. acknowledges the partial financial support from Belarusian Republican Foundation for Fundamental Research under Grant No. F08M-122. A.A.L. acknowledges financial support from Alexander von Humboldt Foundation.

*Corresponding author; gap@bntu.by

[1] L. E. Brus, J. Chem. Phys. **80**, 4403 (1984).
[2] A. P. Alivisatos, Science **271**, 933 (1996).
[3] A. I. Ekimov, Al. L. Efros, and A. A. Onushchenko, Solid State Commun. **56**, 921 (1985).
[4] C. de Mello Donegá, P. Liljeroth, and D. Vanmaekelbergh, Small **1**, 1152 (2005).
[5] V. I. Klimov, Science **290**, 314 (2000).
[6] E. U. Rafailov, M. A. Cataluna, and W. Sibbett, Nat. Photonics **1**, 395 (2007).
[7] A. M. Malyarevich, K. V. Yumashev, and A. A. Lipovskii, J. Appl. Phys. **103**, 081301 (2008).
[8] M. Bruchez, Jr., M. Moronne, P. Gin, S. Weiss, and A. P. Alivisatos, Science **281**, 2013 (1998).
[9] W. J. M. Mulder, R. Koole, R. J. Brandwijk, G. Storm, P. T. K. Chin, G. J. Strijkers, C. de Mello Donegá, K. Nicolay, and A. W. Griffioen, Nano Lett. **6**, 1 (2006).
[10] D. R. Larson, W. R. Zipfel, R. M. Williams, S. W. Clark, M. P. Bruchez, F. W. Wise, and W. W. Webb, Science **300**, 1434 (2003).
[11] F. Wang, W. B. Tan, Y. Zhang, X. Fan, and M. Wang, Nanotechnology **17**, R1 (2006).
[12] X. Michalet, F. F. Pinaud, L. A. Bentolila, J. M. Tsay, S. Doose, J. J. Li, G. Sundaresan, A. M. Wu, S. S. Gambhir, and S. Weiss, Science **307**, 538 (2005).
[13] B. N. G. Giepmans, S. R. Adams, M. H. Ellisman, and R. Y. Tsien, Science **312**, 217 (2006).
[14] O. Madelung, *Semiconductors: Data Handbook*, 3rd ed. (Springer, Berlin, 2004).
[15] J. E. Murphy, M. C. Beard, A. G. Norman, S. Ph. Ahrenkiel, and J. C. Johnson, P. Yu, O. I. Mii, R. J. Ellingson, A. J. Nozik, J. Am. Chem. Soc. **128**, 3241 (2006).
[16] I. Kang and F. W. Wise, J. Opt. Soc. Am. B **14**, 1632 (1997).
[17] J. M. An, A. Franceschetti, and A. Zunger, Nano Lett. **7**, 2129 (2007).
[18] M. Nirmal, D. J. Norris, M. Kuno, M. G. Bawendi, A. L. Efros, and M. Rosen, Phys. Rev. Lett. **75**, 3728 (1995).
[19] A. L. Efros, M. Rosen, M. Kuno, M. Nirmal, D. J. Norris, and M. Bawendi, Phys. Rev. B **54**, 4843 (1996).
[20] R. Espiau de Lamaëstre, H. Bernas, D. Pacifici, G. Franzó, and F. Priolo, Appl. Phys. Lett. **88**, 181115 (2006).
[21] L. Turyanska, A. Patana, M. Heniniet, B. Hennequin, and N. R. Thomas, Appl. Phys. Lett. **90**, 101913 (2007).
[22] D. Valerini, A. Creti, M. Lomascolo, L. Manna, R. Cingolani, and M. Anni, Phys. Rev. B **71**, 235409 (2005).
[23] A. Narayanaswamy, L. F. Feiner, and P. J. van der Zaag, J. Phys. Chem. C **112**, 6775 (2008).
[24] P. Jing, J. Zheng, M. Ikezawa, X. Liu, S. Ly, X. Kong, J. Zhao, and Y. Masumoto, J. Phys. Chem. C **113**, 13545 (2009).
[25] A. A. Onushchenko, A. A. Zhilin, G. T. Petrovskii, E. L. Raaben, M. S. Gaponenko, A. M. Malyarevich, K. V. Yumashev, and V. V. Golubkov, J. Opt. Technol. **73**, 576 (2006).
[26] A. M. Malyarevich, V. G. Savitski, P. V. Prokoshin, N. N. Posnov, K. V. Yumashev, E. Raaben, and A. A. Zhilin, J. Opt. Soc. Am. B **19**, 28 (2002).
[27] K. K. Nanda, F. E. Kruis, H. Fissan, and S. N. Behera, J. Appl. Phys. **95**, 5035 (2004).
[28] E. P. Petrov, J. V. Kruchenok, and A. N. Rubinov, J. Fluoresc. **9**, 111 (1999).
[29] M. J. Fernee, P. Jensen, and H. Rubinsztein-Dunlop, J. Phys. Chem. C **111**, 4984 (2007).
[30] S. W. Clark, J. M. Harbold, and F. W. Wise, J. Phys. Chem. C **111**, 7302 (2007).
[31] L. Turyanska, U. Elfurawi, M. Li, M. W. Fay, N. R. Thomas, S. Mann, J. H. Blokland, P. C. M. Christianen, and A. Patan, Nanotechnology **20**, 315604 (2009).
[32] J. J. Peterson and T. D. Krauss, Nano Lett. **6**, 510 (2006).
[33] H. Kamisaka, S. V. Kilina, K. Yamashita, and O. V. Prezhdo, Nano Lett. **6**, 2295 (2006).
[34] L. A. Padilha, A. A. R. Neves, C. L. Cesar, L. C. Barbosa, and C. H. B. Cruz, Appl. Phys. Lett. **85**, 3256 (2004).
[35] Y.-N. Hwang, C. M. Kim, S. C. Jeoung, D. Kim, and S.-H. Park, Phys. Rev. B **61**, 4496 (2000).
[36] V. Klimov, P. H. Bolivar, and H. Kurz, Phys. Rev. B **53**, 1463 (1996).
[37] M. Jones, S. S. Lo, and G. D. Scholes, J. Phys. Chem. C **113**, 18632 (2009).
[38] A. M. Kapitonov, A. P. Stupak, S. V. Gaponenko, E. P. Petrov, A. L. Rogach, and A. A. Eychmüller, J. Phys. Chem. B **103**, 10109 (1999).
[39] E. P. Petrov, F. Cichos, and C. von Borczyskowski, J. Lumin. **119-120**, 412 (2006).
[40] Y. Nonoguchi, T. Nakashima, and T. Kawai, J. Phys. Chem. C **111**, 11811 (2007).
[41] N. B. Pendyala and K. S. R. K. Rao, J. Lumin. **128**, 1826 (2008).
[42] B. Segall, in *Proceedings of the IX Conference on the Physics of Semiconductors*, Moscow, 1968, edited by S. M. Ryvkin (Nauka, Leningrad, 1968), p. 425; S. Rudin, T. L. Reinecke, and B. Segall, Phys. Rev. B **42**, 11218 (1990).
[43] J. Lee, E. S. Koteles, and M. O. Vassell, Phys. Rev. B **33**, 5512 (1986).
[44] F. Gindele, K. Hild, W. Langbein, and U. Woggon, J. Lumin. **87-89**, 381 (2000).
[45] T. D. Krauss and F. W. Wise, Phys. Rev. Lett. **79**, 5102 (1997).
[46] T. D. Krauss and F. W. Wise, Phys. Rev. B **55**, 9860 (1997).
[47] G. Morello, M. De Giorgi, S. Kudera, L. Manna, R. Cingolani, and M. Anni, J. Phys. Chem. C **111**, 5846 (2007).
[48] A. Kigel, M. Brumer, G. I. Maikov, A. Sashchiuk, and E. Lifshitz, Small **5**, 1675 (2009).
[49] D. M. Sagar, R. R. Cooney, S. L. Sewall, E. A. Dias, M. M. Barsan, I. S. Butler, and P. Kambhampati, Phys. Rev. B **77**, 235321 (2008).
[50] K. Oshiro, K. Akai, and M. Matsuura, Phys. Rev. B **66**, 153308 (2002).
[51] X. Lu, J. Vaillancourt, and H. Wen, Appl. Phys. Lett. **96**, 173105 (2010).
[52] G. Ortner, M. Schwab, M. Bayer, R. Pässler, S. Fafard, Z. Wasilewski, P. Hawrylak, and A. Forchel, Phys. Rev. B **72**, 085328 (2005).
[53] Y. P. Varshni, Physica (Amsterdam) **34**, 149 (1967).
[54] *Non-Tetrahedrally Bonded Elements and Binary Compounds I*, Landolt-Börnstein, New Series, Group III: Condensed Matter Vol. 41, Pt. C, edited by O. Madelung, U. Rossler, and M. Schulz (Springer-Verlag, Berlin, 1998).
[55] A. Olkhovets, R. C. Hsu, A. Lipovskii, and F. W. Wise, Phys. Rev. Lett. **81**, 3539 (1998).
[56] K. P. O'Donnell and X. Chen, Appl. Phys. Lett. **58**, 2924 (1991).
[57] B. L. Wehrenberg, C. Wang, and P. Guyot-Sionnest, J. Phys. Chem. B **106**, 10634 (2002).

[58] J. H. Warner, E. Thomsen, A. R. Watt, N. R. Heckenberg, and H. Rubinsztein-Dunlop, Nanotechnology **16**, 175 (2005).
[59] Y. Chen, D. Yu, B. Li, X. Chen, Y. Dong, and M. Zhang, Appl. Phys. B **95**, 173 (2009).
[60] G. Allan and C. Delerue, Phys. Rev. B **70**, 245321 (2004).
[61] J. C. Johnson, K. A. Gerth, Q. Song, J. E. Murphy, and A. J. Nozik, Nano Lett. **8**, 1374 (2008).
[62] C. de Mello Donegá, M. Bode, and A. Meijerink, Phys. Rev. B **74**, 085320 (2006).
[63] O. Labeau, P. Tamarat, and B. Lounis, Phys. Rev. Lett. **90**, 257404 (2003).
[64] S. A. Crooker, T. Barrick, J. A. Hollingsworth, and V. I. Klimov, Appl. Phys. Lett. **82**, 2793 (2003).